Comparative evaluation of machine learning model and PAP/CAR approach for water erosion prediction in the Beht watershed, Morocco

Ferdaouss Lakhili[1] , Fahed El Amarty[2*] , Afaf Chakir[3], Youssef Hattafi[2],
Nabil Fikri[2], Lahcen Benaabidate[2], Abderrahim Lahrach[2]

[1] Laboratory of Intelligent Systems, Energy, and Sustainable Development (SIEDD), Private University of Fez, Lotissement Quaraouiyine Route Ain Chkef, Fès 30000, Morocco
[2] Functional Ecology and Environmental Engineering Laboratory (LEFGE), FST-Fes, Sidi Mohammed Ben Abdellah University, Immouzer Road, BP: 2202, Fez 30000, Morocco
[3] Laboratory of Innovative Materials and Mechanical Manufacturing Processes (IMMM), ENSAM-Meknes, Moulay Ismail University, Marjane 2, BP: 15290 Meknes 50500, Morocco
* Corresponding author's e-mail: fahed.elamarty@usmba.ac.ma

ABSTRACT

Soil erosion is a major environmental concern, particularly in hydrologically unstable regions. Reliable prediction methods are essential for effective erosion risk assessment and mitigation. This study evaluates and compares two erosion prediction methodologies in the Beht watershed in Morocco – the traditional PAP/CAR model and an advanced machine learning technique, Extreme Gradient Boosting (XGBoost). Using geographic information systems (GIS) and remote sensing data, we integrate various conditioning factors such as slope, elevation, rainfall intensity, and land cover. While the PAP/CAR model provides a qualitative assessment of erosion susceptibility, its limitations in spatial precision necessitate a comparison with data-driven approaches. The results indicate that the PAP/CAR model identifies high-risk erosion zones covering approximately 42.37% of the watershed, but it tends to overestimate spatial distributions. In contrast, the XGBoost model, trained on 70% of inventory data and validated on the remaining 30%, achieves an accuracy of 90.02%, a Kappa coefficient of 0.6, and an AUC-ROC score of 0.96, demonstrating its superior predictive power. By leveraging optimized hyperparameters, XGBoost enhances classification stability, reducing bias and variance, thereby improving model reliability. These findings emphasize the necessity of integrating advanced computational techniques into geospatial analyses for erosion risk management, offering more precise tools for soil conservation strategies and watershed management.

Keywords: PAP/CAR, extreme gradient boosting, cross validation, GIS, machine learning, Beht watershed, water erosion, Morocco.

INTRODUCTION

Soil erosion is a critical environmental issue that degrades land resources due to natural forces such as rain, wind, water flow, ice, and other environmental agents. This process involves various mechanisms, including ablation, sediment transport, scouring, and mass movements. Water-driven erosion occurs when water acts on vulnerable soils, a process influenced by the composition of the substrate, the shape of the terrain, the presence

of vegetation, and agricultural practices (Chalise et al., 2019; Maidment 1993; Kusi et al., 2023). The accurate prediction of erosion-prone areas is crucial for sustainable land and water resource management, as uncontrolled soil loss leads to significant agricultural and hydrological consequences.

To assess susceptibility to erosion and pinpoint high-risk zones, it is essential to analyze key contributing factors such as climatic intensity, particularly precipitation, soil erodibility, topographical features (such as slope steepness),

land use, and vegetation density. Traditional erosion models, including empirical and conceptual approaches, have been widely used, yet they often lack adaptability to local conditions and rely on predefined assumptions that may not always reflect real-world erosion dynamics. Effectively tackling this issue today requires the adoption of cutting-edge techniques and sophisticated geographic information management tools (Pelletier, 2012; Arnoldus, 1980; Gebrehiwot et al., 2014; Hilmi et al., 2023; Ozer et al., 2020).

To estimate water erosion, a variety of predictive models and assessment methods have been developed worldwide. These models are categorized into three main types: empirical, physical, and conceptual, with the choice depending primarily on data availability. Among these, the revised universal soil loss equation (RUSLE) model has been widely used for mapping and simulating water erosion, demonstrating high reliability (Achu and Thomas 2023; Ahmad et al., 2023; Ashiagbor et al., 2012; 2013; Boissy et al., 2022; EL Hadi, 2014). In Morocco, several studies utilizing GIS tools have applied this model to analyze erosion patterns. Research focused on erosion modeling and its underlying causes(Tabyaoui et al. 2016; Elkadiri et al. 2014; Sadiki,A et al. 2012; El Amarty et al. 2024) has been carried out in the Oued Haricha, Oued Lkhmiss, and Oued Boussouab catchments, where estimated soil losses reach 62.72 t/ha/yr, 36 t/ha/yr, and 55.35 t/ha/yr, respectively.

Another widely used approach for mapping and modeling soil erosion is the PAP/CAR method, which has proven effective in numerous studies (Tahouri et al., 2022; Tahouri et al., 2019; Lahlaoi et al., 2015; Yacine et al., 2019). In Morocco, GIS-based research has incorporated this methodology to assess watershed susceptibility to erosion hazards. For instance, (Mesrar et al., 2015) applied the PAP/CAR framework in the Sahla watershed to evaluate erosion processes and their contributing factors. Likewise, (Boukrim et al., 2016) employed this method to produce qualitative erosion maps for the Aoudour watershed in the Rif region of Morocco. Despite its widespread application, the PAP/CAR approach remains a deterministic model with predefined classification rules, limiting its predictive accuracy in heterogeneous landscapes.

Before implementing soil conservation strategies, a comprehensive spatial evaluation of erosion risk is necessary (Akalai et al. 2014; Basharat et al. 2014; Duchemin et al. 2005; Efiong et al. 2021). However, traditional models face challenges in capturing the complexity of erosion dynamics, necessitating the integration of data-driven methods such as machine learning. Recent advancements in artificial intelligence have enabled the development of predictive models capable of capturing intricate relationships between multiple environmental variables.

This study aims to compare the predictive performance of a traditional deterministic approach (PAP/CAR) with a machine learning model (XGBoost) for water erosion assessment in the Beht watershed, Morocco. By leveraging remote sensing and GIS, this research seeks to:
- Evaluate the efficiency of PAP/CAR in erosion risk assessment and identify its limitations.
- Assess the predictive capabilities of the XGBoost model, trained on diverse environmental conditioning factors.
- Determine whether machine learning techniques can enhance the accuracy and spatial resolution of erosion risk prediction compared to traditional models.

By addressing these research questions, this study contributes to bridging the gap between traditional erosion assessment methods and modern computational techniques, offering insights into the applicability of AI-based approaches for soil conservation and watershed management.

METHODS AND MATERIALS

The area study

The Oued Beht watershed, covering an area of 4.432 km², is situated upstream of the El Kansera dam. It extends in a northwest-southeast direction and is bordered to the north by Sidi Kacem and Sidi Slimane, to the northeast by Mèknes, to the east by El Hajeb, Ifrane, and Jbel Hebri, to the south by Mrirt and Oued Oum Rabia, and to the west by the urban centers of Oulmes and Khemisset. This watershed is a sub-basin of the larger Oued Sebou watershed. The hydrographic network originates in the central-northern region of Morocco and the western Middle Atlas. The river merges with the lower Oued Sebou after passing through the central southern Rifain furrow, where it receives significant contributions from various tributaries. It then traverses the Prérif and the southern part of the El Gharb plain, which is part of the western southern Rifain furrow (Fig. 1).
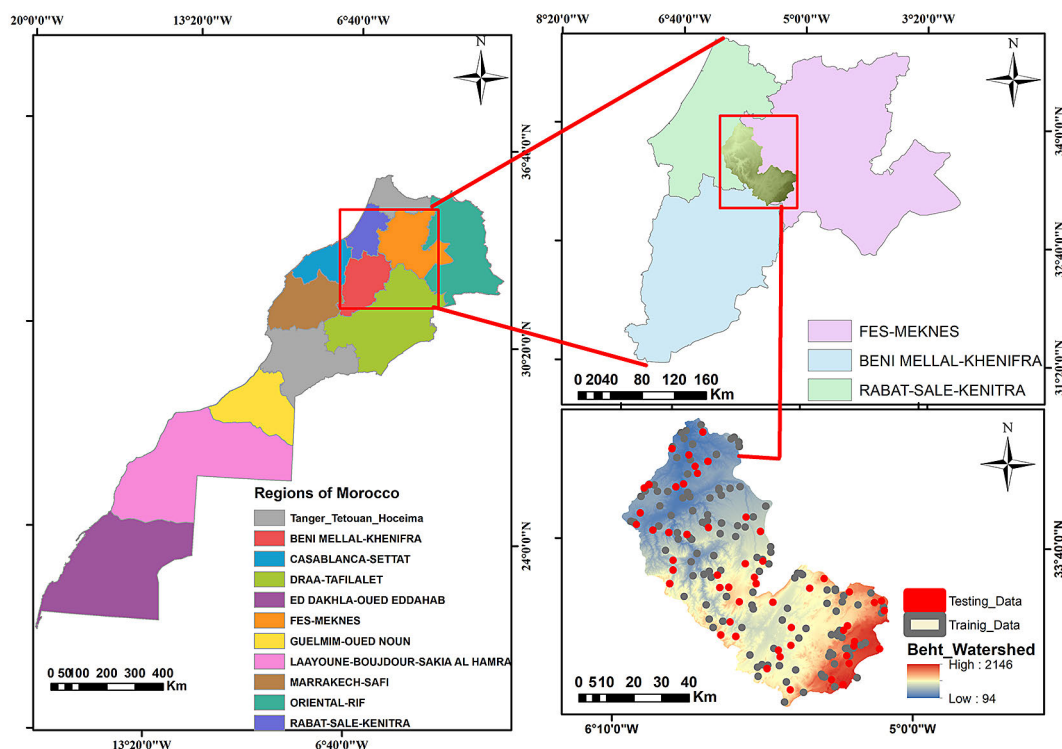
Figure 1. Oued Beht watershed location

Geologically, the watershed comprises formations ranging from the Paleozoic to the Quaternary periods. The Paleozoic basement and its sedimentary cover are overlain by Upper Miocene deposits in the southern Rifain furrow. The Oued Beht fluvial terraces, consisting of tiered and nested deposits, rest unconformably on the Miocene substratum. The watershed spans three major geological and structural units: Central Hercynian Morocco (Ait Yacine et al. 2019; Hilmi et al. 2023; HCEFLCD 2014; Lakhili et al. 2017), the Middle Atlasic Causse, and the South Rifain Sillon. It is predominantly composed of impermeable formations from the Primary and Permo-Triassic periods of the Massif Central. Quaternary basalts, present in some areas along the Oued Beht, are of minor geological significance (Hilmi et al. 2023). The Paleozoic complex, consisting mainly of Ordovician, Silurian, and Carboniferous formations, is dominated by shales interspersed with occasional layers of quartzite and limestone. Further north, upstream from El Kansera, Permo-Triassic red saliferous clays are found alongside small basalt outcrops of limited extent.

The region experiences a Mediterranean climate characterized by two distinct seasons: a wet, cold period and a dry, hot period. Annual precipitation averages around 700 mm across the basin, though rainfall distribution is highly irregular, both seasonally and interannually. Rainfall events are often convective in nature, leading to thunderstorms that can trigger severe flooding.

Methodologies and data sets

The qualitative evaluation of water erosion using the PAP/CAR model relies on an integrated analysis of risk-inducing factors, requiring a cartographic methodology combined with data processing and interpretation. This approach is structured around three complementary components.

The predictive component focuses on thematic mapping of key factors influencing erosion, such as lithology, slope gradient, land use, and vegetation density. The objective is to delineate homogeneous erosion-prone zones and develop a cartographic representation of erosion patterns. This process involves multiple sequential steps, including generating slope and lithology maps, producing friability and erodibility maps by overlaying slope and lithofacies data, and creating land use and vegetation cover maps derived from Landsat-8 satellite imagery. Additionally, a soil protection map is constructed by combining land use and vegetation cover density data,

while the final thematic map of erosive conditions is obtained by integrating the erodibility and soil protection layers.

The descriptive component aims to assess and map existing erosion processes, providing insight into ongoing soil degradation and the extent of exposure to erosion. Meanwhile, the integrative component synthesizes findings from both the predictive and descriptive approaches to generate a comprehensive map of erosion trends. This synthesis enables the evaluation of erosion dynamics by categorizing areas based on erosion intensity and susceptibility levels. The model's input parameters are combined following the PAP/CAR framework, which was developed through extensive studies across various Mediterranean regions to establish correlations between different erosion-driving factors.

The PAP/CAR methodology is extensively utilized across several regions in the Rif and Middle Atlas, particularly within the watersheds of Amzaz, Oued Zgane, Sahla, Kharouba, Oued Beht, Oued Larbaa, and Assfalou (Iaaich et al., 2016; Ousmana et al., 2017; Mohajane et al., 2021; Dallahi et al., 2021; Sadiki et al., 2012; Tahouri et al., 2022). However, an evaluation of the results reveals certain shortcomings, such as the overestimation of the spatial distribution of erosion risk zones. To enhance the accuracy of these estimates, this study incorporates machine learning algorithms, specifically Extreme Gradient Boosting to refine the prediction of water erosion hazard patterns within the study area. The focus is on sheet erosion, with the results compared to those obtained from conventional PAP/CAR modeling, represented by the water erosion trend map, to assess the contribution of machine learning techniques in improving predictive accuracy.

The data used in this research come from various sources, including a digital elevation model (DEM), a Landsat 8 satellite image captured on June 30, 2024, and an inventory of sheet erosion patterns documented in the study area up until March 2025. Data preprocessing involves several stages: (i) initial processing of the DEM and Landsat 8 image in the ArcGIS environment. (ii) extraction of topographic and climatic variables, as well as factors derived from the RUSLE equation.(iii) preparation of the sheet erosion inventory for modelling (Table 1), and (iv) selection of training and testing datasets using a random sampling method, with 70% of the data allocated for training and 30% for testing (Fig. 2).

As previously outlined, the validation procedure involved splitting the inventory data into two separate groups: 70% of the data was allocated for training the model, and the remaining 30% was reserved for testing the model's performance. Out of 180 total inventory points, 126 were used for training, and 54 were set aside for validation (Fig. 3). To evaluate the effectiveness of the statistical model, along with estimating its variance and bias, the training set underwent a resampling technique called cross-validation (CV).

Cross-validation is a widely adopted approach in classification tasks to assess the reliability of a statistical model. This method divides the dataset into distinct subsets designated for training and testing, ensuring balanced sampling and minimizing the chances of overfitting or underfitting during the model's optimization. In this analysis, 10-fold cross-validation (10-fold CV)

Table 1. Characteristics of predisposing factors to modeling Sheet erosion

| Data	Resolution / Scale	Source
DEM	30 × 30	https://earthexplorer.usgs.gov
Landsat 8	30 × 30	https://earthexplorer.usgs.gov
Elevation	30 × 30	Derived from the DEM
Slope	30 × 30	Derived from the DEM
Aspect	30 × 30	Derived from the DEM
Factor_R	30 × 30	Rango and Arnoldus Eq (1987)
Factor_LS	30 × 30	Mitasova et al. Eq (1996)
Factor_K	30 × 30	Williams Eq (1995)
Factor_C	30 × 30	De Jong Eq (1994)
LULC	30 × 30	Derived from the Landsat 8
Cover_Density	30 × 30	Derived from the Landsat 8
Lithology	1/50000, Rasterization 30 × 30	digitization of geologic maps 1/50000
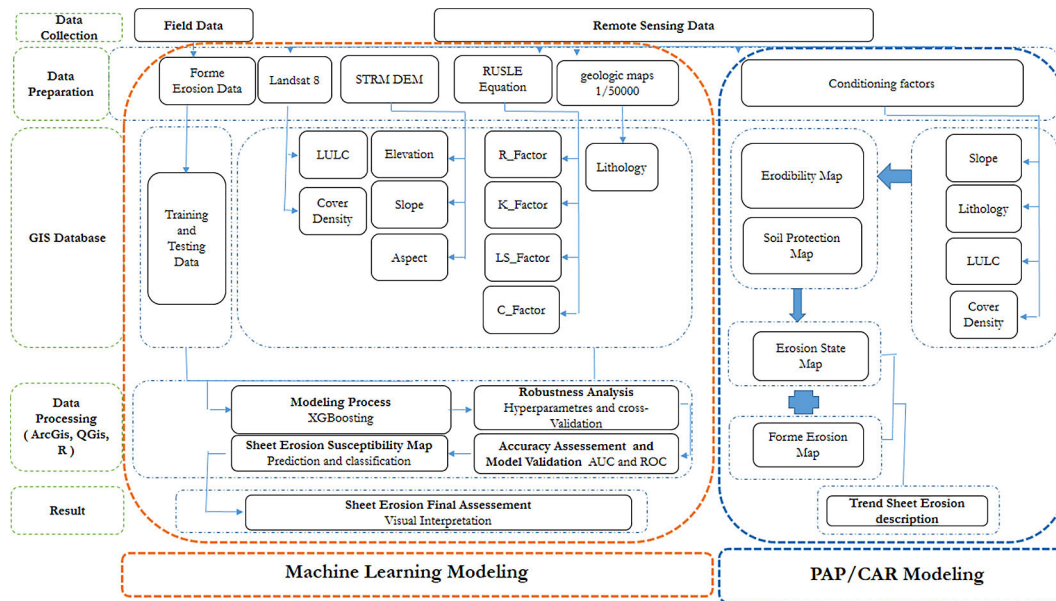
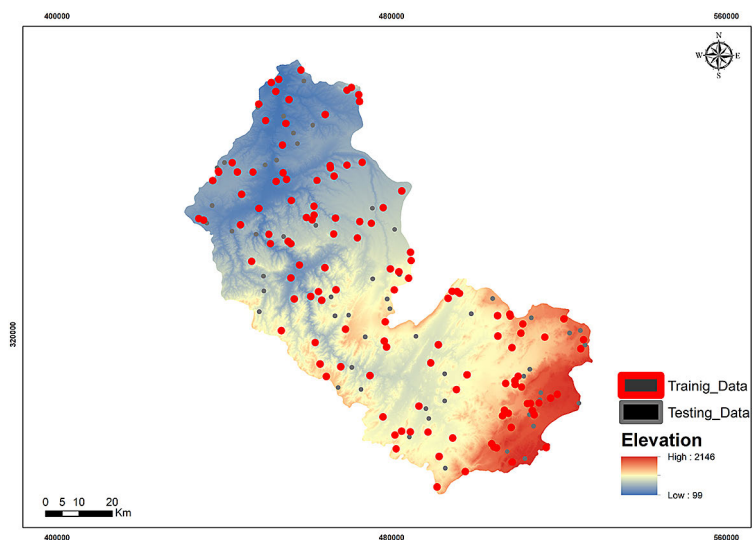**Figure 2.** Flowchart of Sheet erosion susceptibility modeling

Figure 3. Sheet erosion inventory map

was employed. The dataset was randomly split into ten equal-sized subsets, or "folds." In each iteration, the model was trained on nine of the folds and validated on the remaining fold. This process was repeated ten times, ensuring that each fold was used once for testing. The final performance of the model was determined by averaging the results from all ten iterations, providing a more robust and reliable assessment of its accuracy.

Conditioning factors of PAP/CAR modeling

An analysis of the slope distribution map (Table 2 and Fig. 4a) for the Oued Beht watershed

reveals that the majority of the study area is characterized by low to moderate slopes, with gradients of less than 12%, which cover approximately 72.53% of the total surface area. Specifically, the low-slope class (0–3%) comprises 29.60% of the basin's surface, translating to 1305.19 km², predominantly situated in the lower-lying regions and the primary river valleys. The moderate slope class (3–12%) extends across 42.93% of the total area, or 1892.74 km², and is spread across most of the watershed, significantly influencing soil stability and surface water runoff dynamics. Steeper slopes (12–20%) account for 21.56% of the total surface area, being concentrated primarily in

Table 2. Slope, LS and erodibility proprieties of Oued Beht watershed

| Slope_class	Slope_Type (%)	Slope_State	Area in km²	Area in %
1	0–3	Low	1305.19	29.60
2	3–12	Moderate	1892.74	42.93
3	12–20	Steep	950.78	21.56
4	20–35	Strong	247.92	5.62
5	> 35	Extreme	12.53	0.28
LS_Class	Lithology_Type	Lithology_state	Area in km²	Area in %
5	Alluvial terraces	Very weak	370.36	8.40
4	Yellow sandy marls	Low	3362.95	76.24
3	Conglomerates, red sandstones	Average	323.99	7.35
2	Red conglomerates,basaltic lavas	Strong	74.55	1.69
1	basalts, ankaratrites	Extreme	279.10	6.33
Erodibility class	Erodibility_type	Erodibility_State	Area in km²	Area in %
1	Low (EN)	Low (EN)	354.22	8.03
2	Moderate (EB)	Moderate (EB)	1196.85	27.13
3	Average (EM)	Average (EM)	1734.01	39.31
4	Strong (EA)	Strong (EA)	874.43	19.82
5	Extreme (EX)	Extreme (EX)	251.38	5.70
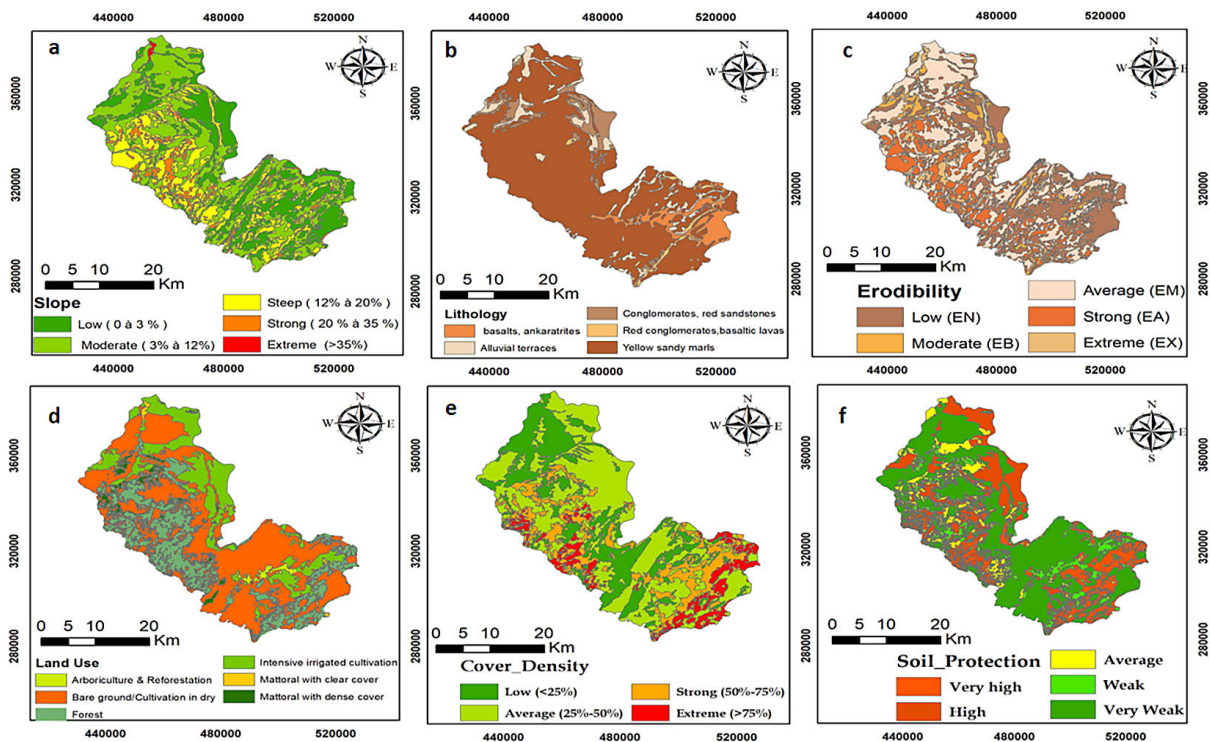
Figure 4. Maps of conditioning factors of Sheet erosion (PAP/CAR modeling): (a) slope, (b) lithology, (c) erodibility, (d) land use, (e) cover density, (f) soil protection

the central and upper portions of the basin. Areas with very steep slopes (20–35%) cover 5.62% of the watershed and are typically found in the mountainous regions where the intensity of water erosion is notably higher. Finally, extreme slopes (> 35%), although comprising only 0.28% of the area, are situated in steep, highly vulnerable zones prone to significant erosion and soil instability.

The Oued Beht watershed exhibits considerable lithological diversity, which plays a crucial role in determining the susceptibility of the area to erosion (Table 2 and Fig. 4b). The most

prevalent formation within the region is yellow sandy marl, covering 76.24% of the total surface area. This material is known for its relatively low mechanical strength, which renders it particularly prone to differential erosion and landslide occurrences. Alluvial terraces, occupying 8.40% of the basin's surface area, are typically found along river channels and are highly susceptible to weathering and erosion due to their minimal resistance. Red conglomerates and sandstones, which cover 7.35% of the surface, exhibit moderate resistance to erosive forces, whereas the red conglomerates and basaltic lavas, which constitute 1.69% of the total area (or 74.55 km²), offer a higher degree of erosion resistance. Finally, basalts and ankaratrites, though covering only 6.33% of the area, represent the most erosion-resistant formations in the region, playing a vital role in maintaining the structural integrity of the landscape.

The erodibility of the Oued Beht watershed is primarily influenced by the nature of the geological materials and the land's slope characteristics (Table 2 and Fig. 4c). Low erodibility zones (EN) cover 8.03% of the total area, predominantly located in regions where resistant geological formations are present and slopes are moderate. These areas exhibit minimal susceptibility to erosion due to the stability of the underlying materials and topography.

Moderately erodible regions (EB) represent 27.13% of the watershed's surface area. These zones are characterized by more pronounced weathering, although the erosion process is still constrained by the structural integrity of the rock formations. In contrast, medium erodibility (ME) areas account for the largest portion of the watershed, encompassing 39.31% of the area. These zones are marked by lithological formations that are relatively sensitive to erosion, compounded by moderate to steep slopes, which create favorable conditions for the development of gullies and sheet erosion.

Highly erodible regions (EA) cover 19.82% of the basin's total area and are particularly vulnerable to water erosion. These areas are typically found in sectors with steep slopes and loose, easily disintegrated materials, making them highly susceptible to erosion processes. Lastly, extreme erodibility (EX) zones, although constituting just 5.70% of the territory, represent the most erosion-prone areas within the watershed. These regions experience rapid soil and sediment removal, leading to geomorphological instability and significantly accelerating erosion processes.

An analysis of land use within the Oued Beht watershed (Fig. 4d) demonstrates a pronounced prevalence of bare soil and dry crops, which together cover 52.36% of the total surface area (Table 3). This land use pattern significantly heightens the watershed's susceptibility to water erosion, as the lack of dense vegetation cover exacerbates the impacts of water abstraction and surface runoff. In contrast, areas dedicated to

Table 3. Land use, cover density and soil protection proprieties of Oued Beht watershed

Land use_class	Land use type	Area in km²	Area in %
1	Arboriculture & Reforestation	44.91	1.01
2	Mattoral with dense cover	151.13	3.41
3	Forest	1050.40	23.69
4	Mattoral with clear cover	25.37	0.57
5	Bare ground/Cultivation in dry	2321.70	52.36
6	Intensive irrigated cultivation	840.22	18.95
Cover density_class	Type and state	Area in km²	Area in %
1	Low < 25%	1230.58	27.90
2	Average 25–50%	2013.15	45.65
3	Strong 50–75%	753.10	17.08
4	Extreme > 75%	413.29	9.37
Soil_protection_class	Soil_protection_state	Area in km²	Area in %
1	Very high	555.93	12.53
2	High	827.26	18.65
3	Average	442.07	9.97
4	Weak	437.91	9.87
5	Very weak	2172.45	48.98

irrigated crops (18.95%) and woodland (23.69%) offer some degree of soil stabilization. However, the distribution of these wooded areas is uneven across the basin, leaving certain regions, particularly in the downstream sections, highly vulnerable to erosion. The limited extent of matorral (3.98%) and reforested areas (1.01%) further emphasizes the scarcity of protective vegetation, intensifying soil fragility in areas subjected to intensive agricultural practices and human activity. These figures point to an insufficient natural buffer against erosion, exacerbating the vulnerability of the watershed's soils.

Further examination of vegetation cover density (Fig. 4e) underscores the uneven distribution of vegetation and its consequent effect on soil stability. The low-density cover class (< 25%) is dominant, covering 27.90% of the area, while 45.65% of the basin is characterized by moderate vegetation density (25–50%), providing only a moderate level of protection against erosion. In contrast, regions with dense vegetation cover (> 50%) account for a mere 26.45% of the total area, with these dense areas primarily concentrated in forested regions. This imbalance results in the concentration of erosion-prone zones in areas with insufficient vegetation, where runoff is more likely to occur and lead to soil degradation. Overall, the fragmentation of vegetation cover across the watershed highlights the urgent need for enhanced soil conservation strategies, such as expanding forested areas and promoting the regeneration of natural vegetation. Such measures would serve to bolster the watershed's resilience to erosive processes and contribute to long-term soil stability.

The integration of these factors into the soil protection assessment (Fig. 4f) reveals a significant dominance of regions with minimal to low protection, which account for 48.98% and 9.87% of the total basin area, respectively. These vulnerable areas, primarily located in agricultural zones and on bare land, face heightened susceptibility to water erosion. Conversely, regions offering moderate to high levels of protection cover a mere 41.15% of the area, underscoring the disparity in the distribution of stabilized land. The findings emphasize the critical need for sustainable land management practices, such as strategic reforestation efforts, agroforestry initiatives, and erosion control measures, to enhance the watershed's resistance to soil degradation.

Conditioning factors of machines learning modeling

The application of machine learning models, particularly XGBoost, to predict water erosion patterns in the Oued Beht watershed incorporates ten key factors that directly affect the susceptibility of soil to erosion. These factors, detailed in Figure 5, encompass a range of climatic, topographical, and environmental parameters, facilitating the accurate modeling of erosion processes. The variation in the erosivity factor, depicted in Figure 5i, reveals a relatively narrow range of values compared to previous studies such as those by Khali Issa et al. (2019) for the Oued Lkhmis catchment in the Western Rif, where values ranged from 87 to 113. In comparison, the erosivity factor in the present study varies between 162 to 192 for Oued Sahla (Central Rif) and 215 to 228 for the Telata catchment. Despite some variation, the results in this study align closely with other regional studies that focus on similar catchments.

Erodibility, which measures soil resistance to erosion, is determined by factors such as soil texture, structure, organic matter, and permeability, all of which influence the K factor (Iaaich et al., 2016; Duiker et al., 2001). In this study, the K factor was computed using the Williams equation, considering the silt, sand, clay, and organic carbon content of the soil. The K values range from 0.17 to 0.81 t·h·ha·ha^{-1}·MJ^{-1}·mm^{-1}, and the map of erodibility indicates that the Oued Beht watershed exhibits a medium vulnerability to erosion, with only 3.5% of the area showing low erodibility (Fig. 5e).

The LS factor, which quantifies the impact of topography on erosion, is influenced by both slope length (L) and slope gradient (S). Slope length is defined as the distance between the runoff source and the point where deposition begins, typically entering a defined drainage channel (Asmare et Hailemariam 2021; Bryan et Poesen 1989). Using the digital terrain model with 30-meter resolution, various formulas, including those from Wischmeier and Smith (1978), were applied to calculate the LS factor. The LS values range from 0 to 107 (Fig. 5f), with these results generally aligning with those observed in the Oued Sahla watershed (ranging from 0.48 to 87.9). In contrast, the LS values found in this study are higher compared to those in the Oued Lkhmiss catchment, where they range from 5 to 55.

The canopy management factor (C) evaluates the rate of soil loss under specific land use conditions, reflecting the influence of agricultural
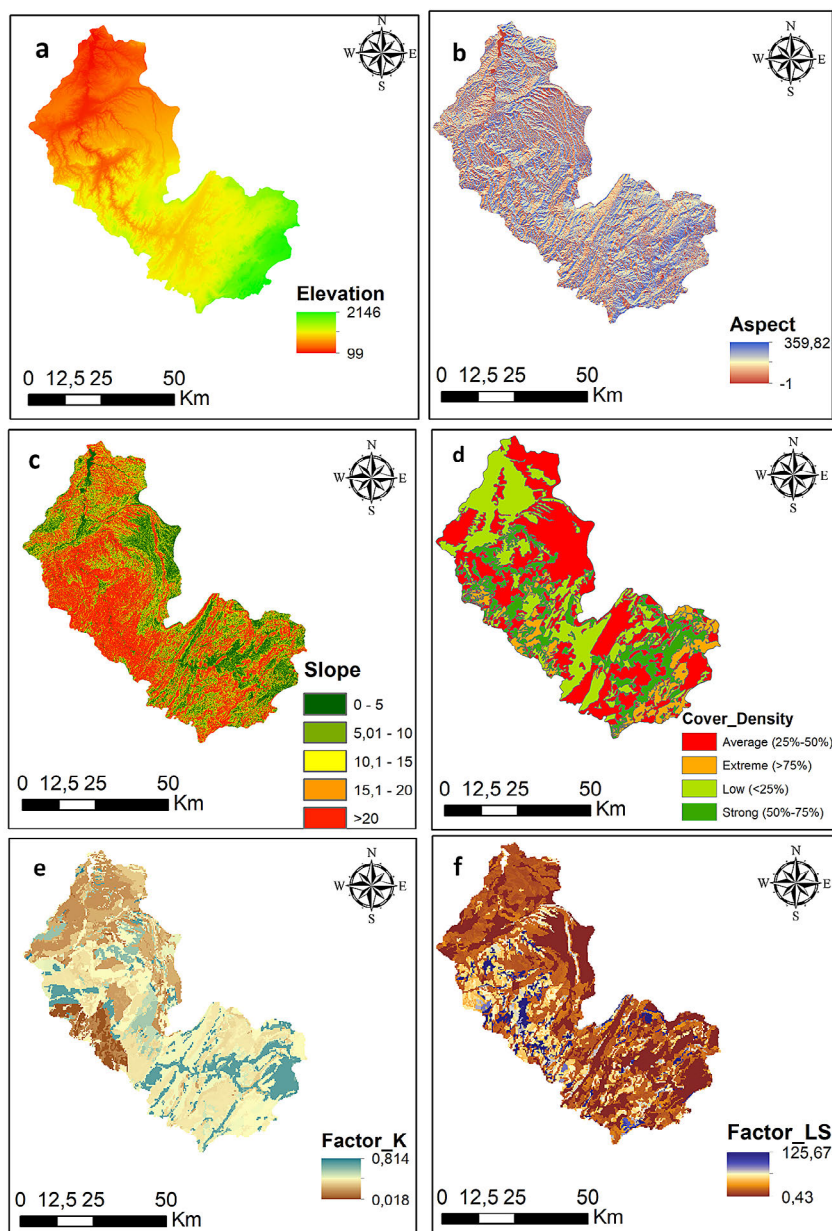
Figure 5. Maps of conditioning factors of Sheet erosion (machine learning modeling): (a) elevation; (b) aspect; (c) slope; (d) cover density; (e) K_factor; (f) LS_factor

and land management practices on erosion. The C factor varies depending on vegetation cover, with higher values indicating poorer cover and higher erosion risks (De Jong, 1994). The C factor map in this study, generated from a Landsat-8 image (June 30, 2024), was complemented by field verification and the calculation of NDVI indices to estimate C-factor values. Using the De Jong equation, the C-factor values show a marked increase in the southeastern portion of the watershed, where intensive agricultural activities and continuous cultivation exacerbate erosion risks. Conversely, the upstream, eastern, and northern areas, characterized by higher altitudes, precipitation,

and forest cover, show lower C values, indicating better soil protection.

Rainfall erosivity, a key factor in water erosion, is the product of total rainfall kinetic energy (E) and the maximum 30-minute rainfall intensity (I30), as outlined by Renard et al. (1997) (Renard et al., 1991; Toy et al., 1999). However, data limitations on rainfall kinetic energy and intensity posed challenges for this study. To address this, we collected precipitation data over 40 years (1983–2023) from various meteorological stations, filling gaps through nearest-neighbor interpolation. The R factor, calculated from monthly and annual precipitation data, was interpolated using
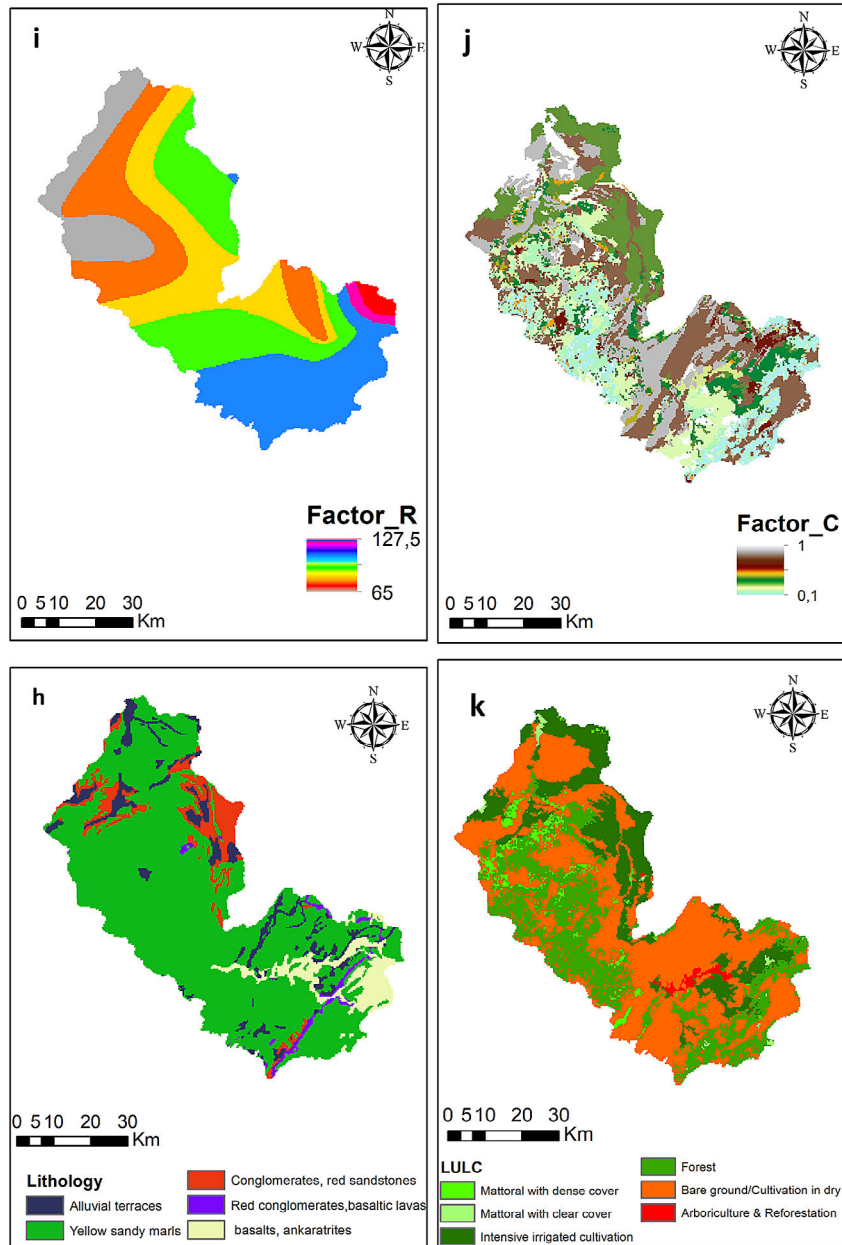
Figure 5. Cont. (i) R_factor; (j) C_factor; (h) lithology, (k) land use

inverse distance-weighted (IDW) methods. The R values for the Oued Beht catchment range from 65 to 127.5 MJ mm ha^{-1} h^{-1} yr^{-1}, with higher values observed in the northern and north-western parts of the watershed, where precipitation is more abundant, and lower values in the southwestern areas, reflecting a decrease in rainfall towards the south.

RESULTS AND DISCUSSIONS

The PAP/CAR erosion trend results from the intersection between the map of erosion states and the map of current erosion patterns in the study area. In contrast, the prediction of erosion patterns using machine learning models results in a sheet erosion susceptibility map, which is the focus of our comparative study. The results obtained are presented in the following sections.

Water erosion trend (PAP/CAR modeling approach)

The erosion status mapping (Fig. 6a) is the result of a comprehensive cartographic analysis that incorporates multiple factors related to soil protection and erodibility. This approach aims to illustrate the intricate interactions between variables influencing water erosion and to classify the watershed into homogeneous zones based on their susceptibility to erosion.
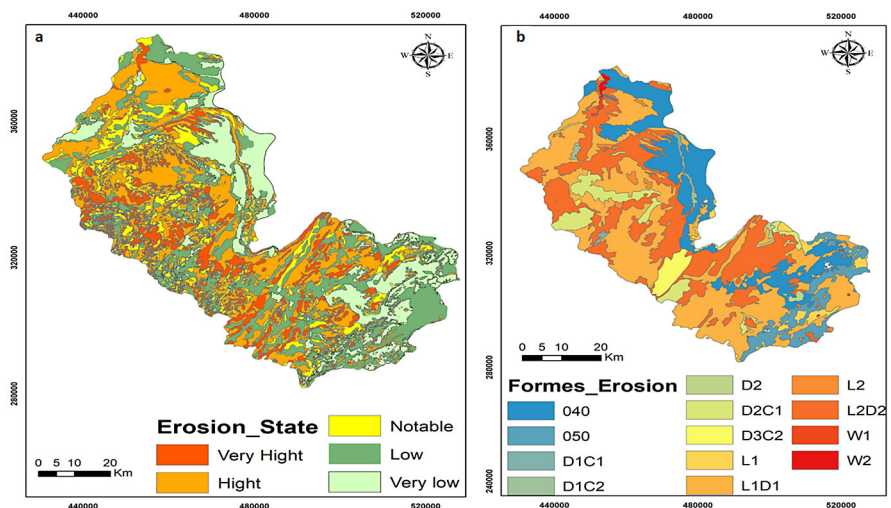
Figure 6. (a) Erosion state and (b) forms erosion Maps of Oued Beht watershed

Table 4. Erosion state and erosion forms proprieties of Oued Beht watershed

Erosion_class	Erosion_state	Area in km²	Area in %
1	Very low	770.62	17.38
2	Low	1139.32	25.69
3	Notable	645.57	14.56
4	Hight	1337.80	30.17
5	Very hight	541.22	12.20
Forme of erosion class	Forme of Erosion_ state	Area in km²	Area in %
1	040	754.69	17.16
2	050	275.06	6.25
3	D1C1	23.31	0.53
4	D1C2	14.57	0.33
5	D2	22.18	0.50
6	D2C1	260.01	5.91
7	D3C2	87.47	1.99
8	L1	91.92	2.09
9	L1D1	1638.59	37.25
10	L2	36.88	0.84
11	L2D2	1174.66	26.70
12	W1	7.97	0.18
13	W2	11.77	0.27

The outcomes of this analysis (Fig. 6a and Table 4) indicate that approximately 42.37% of the watershed is subject to severe erosion, represented by two high-risk categories: high and very high risk, encompassing areas of 1,337.80 km² and 541.22 km², respectively. These highly eroded regions are predominantly located on steep terrains where vegetation is either degraded or absent, with significant occurrences of bare soil and badlands. In contrast, regions with low to very low erosion risk constitute 43.07% of the total watershed area (1,909.94 km²). These zones are mainly situated in the upper and middle sections of the watershed, where vegetation is more intact, including dense forests and matorral. Additionally, these areas are characterized by geological formations that are relatively resistant to erosion, composed of cohesive rock types. The class representing moderate erosion risk, covering 14.56% of the watershed (645.57 km²), is more dispersed across the region. These areas typically occur on moderate slopes (< 35%), where the soils are moderately weathered and have low cohesion. This category is often associated with cultivated land, including fruit tree

plantations and perennial crops, particularly those located along watercourses.

The Oued Beht watershed exhibits a range of erosive processes, primarily influenced by the relief's topography, the lithological composition, and the density of vegetation cover. The erosion map (Fig. 6b) results from a synthesis of satellite image analysis and ground-truthing. Spatial assessment of erosion forms within the watershed reveals a clear dominance of sheet erosion (L1) and surface gullying (D2), which account for 37.25% and 26.70% of the total area, respectively. These erosion types are particularly prevalent along riverbanks and in areas experiencing high runoff, where the soils, predominantly composed of marl and friable materials, are highly prone to erosion. The interaction between surface runoff and human activities further exacerbates these processes, contributing to their rapid expansion. These findings align with those from similar regions in the Central Rif, such as the Oued Aoudour watershed, and the Tabular Middle Atlas, particularly in the Oued Zgane watershed, where comparable geomorphological and climatic factors have resulted in analogous erosion dynamics.

The distribution of deeper gullies, including moderate (D3C2) and superficial (D2C1) forms, covers relatively limited areas within the watershed, accounting for 1.99% and 5.91%, respectively. These types of erosion are predominantly found in areas with steep slopes, where the concentration of runoff significantly contributes to the formation of gullies and ravines. In contrast, more advanced forms of linear erosion, such as L2 and L2D2, collectively cover approximately 27.54% of the total watershed area. These erosion types are indicative of more intense erosive processes, typically occurring in zones where soil stability is weakened due to low material cohesion and sparse vegetation cover. Lastly, deep and moderately deep gullies (C1, C2, and C3) are relatively rare, occupying 0.53%, 0.33%, and 0.50% of the watershed, respectively. These forms of erosion are predominantly located in the southeastern portion of the basin and a few upstream sectors. Their occurrence suggests more advanced erosion in localized areas, where the interplay between slope, soil composition, and runoff intensity creates ideal conditions for the development of such features.

Sheet erosion in the Oued Beht watershed exhibits a spatially heterogeneous distribution, influenced by topographic characteristics and land cover. In the upstream areas, mainly located in the south and southeast, sheet erosion is relatively limited due to the presence of a denser vegetation cover, consisting mainly of forest formations and matorral. These high-altitude zones also benefit from more resistant geological formations, which help reduce surface particle detachment. However, some localized sectors on steeper slopes show signs of sheet erosion, particularly in areas affected by deforestation and overgrazing.

In the central part of the watershed, which includes the northeast and northwest regions, sheet erosion becomes more pronounced, especially on intermediate slopes where the gradient is moderate to steep. This zone is characterized by a mix of cultivated lands and bare soils, which facilitates the mobilization of surface particles by runoff. Erosion is particularly intense in areas dominated by marl and clay formations, as these weakly cohesive substrates are highly susceptible to water erosion.

Finally, in the downstream part of the watershed, mainly in the north, sheet erosion tends to decrease due to the gentler terrain and the progressive sedimentation of materials transported from upstream. However, certain areas near watercourses and alluvial plains still show signs of diffuse erosion, particularly in agricultural zones where land management practices do not always provide effective soil protection against runoff. These observations highlight an erosion dynamic driven by the interaction between relief, soil type, and vegetation cover, with a decreasing intensity of sheet erosion from intermediate slopes towards the floodplain areas.

Sheet erosion susceptibility mapping using XGBoost (machine learning modeling approach)

Hyperparameter impact on model performance

Figure 7 presents a scatter matrix illustrating the interaction between the various hyper parameters of the tested XGBoost model. The objective of this analysis is to identify the optimal combinations that enhance model performance, measured by Accuracy and Kappa.

The detailed results in the hyperparameter table indicate that the best configuration corresponds to eta = 0.05, max_depth = 22, gamma = 0, colsample_bytree = 1, min_child_weight = 2, and subsample = 0.5, with the number of iterations set to 200. This configuration achieved a maximum Accuracy of 0.9002 and a Kappa of 0.6004, indicating a significant improvement compared to other
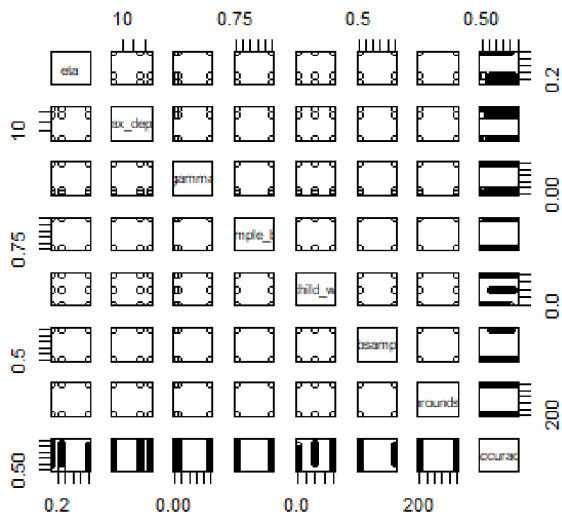
Figure 7. Hyper_ parameters of XGBoost model

tested configurations. Conversely, certain combinations, particularly those with high eta values (≥ 0.3) and shallow tree depth (max_depth ≤ 6), led to lower performance, with a minimum Accuracy of 0.6971 and a negative Kappa of -0.0066, indicating the model's inefficacy under these conditions.

The impact of subsample and colsample_bytree is also evident: partial data and column sampling (subsample = 0.5 and colsample_bytree = 0.75) tend to enhance model robustness by limiting overfitting. However, an excessive reduction in these values leads to performance degradation. The min_child_weight parameter also influences model stability: a higher value (min_child_weight = 2) appears to promote better generalization of predictions. Finally, a second optimization was conducted by fixing the best-performing hyper parameter values: eta = 0.05, max_depth = 6, gamma = 0.1, colsample_bytree = 0.75, min_child_weight = 1, subsample = 1, and nrounds = 200. This configuration resulted in an Accuracy of 0.8469 and a Kappa of 0.1931, slightly lower than the previously obtained maximum performance but offering greater stability, with a reduced AccuracySD of 0.1584.

Variable importance in the optimized XGBoost model

Figure 8 illustrates the importance of the variables used in the XGBoost model after a complete hyper parameter optimization. The objective of this analysis is to identify the most influential factors in predicting the studied phenomenon. The results show that slope is the most significant variable, followed by elevation. This dominance can be explained by the fact that slope directly influences erosion and runoff processes, while elevation can serve as an indirect indicator of the topographic and climatic conditions of the study area.

The parameters of the revised universal soil loss equation, exhibit-varying levels of importance. Among them, Factor_LS is the most influential, supporting the idea that terrain morphology plays a key role in the studied phenomenon. Factor_K and Factor_R show moderate influence, suggesting that soil resistance to erosion and rainfall intensity have a notable but lesser impact compared to topographic variables. In contrast, Factor_C, which represents the effect of vegetation cover, has relatively low importance, possibly due to a homogeneous vegetation cover in the study area.

Other variables, such as lithology and cover density, have a weaker influence, indicating that their contribution to the prediction is less significant compared to topographic and climatic factors. Finally, the classes of the Aspect parameter (I1, I3, I5, I6) appear to be the least influential in the model, suggesting that slope orientation has a limited impact on the studied phenomenon. This low importance may be explained by the lack of a strong correlation between terrain orientation and the processes at play in the study area.

These results confirm that topographic factors (slope, elevation, LS) are the primary determinants of the modeled phenomenon, while erosion-related parameters (RUSLE factors) have a secondary yet non-negligible contribution. Analyzing variable importance helps optimize the selection of parameters to include in the model and enhances its predictive robustness.
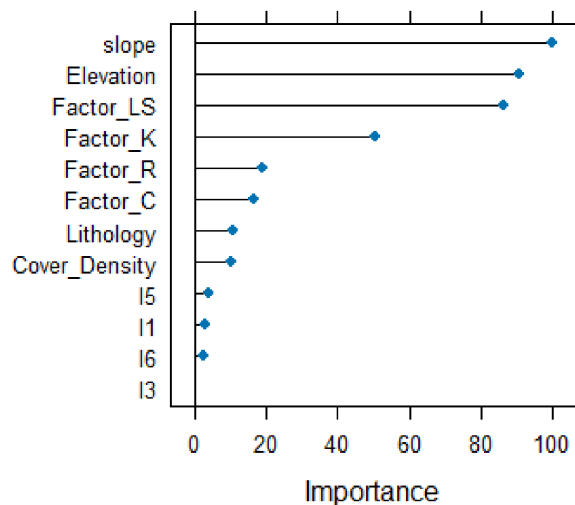

Figure 8. Variable importance in the optimized XGBoost model

ROC curve for the optimized XGBoost model

The performance and reliability assessment of the XGBoost model is based on the analysis of the Receiver Operating Characteristic curve and the Area under the Curve value. As shown in Figure 9, the optimized model achieves an AUC of 0.96 on the test dataset, demonstrating its strong discriminatory power. This high performance is attributed to the rigorous selection of conditioning factors and the optimal tuning of hyper parameters, ensuring effective classification and improved prediction of high-risk areas.

The most influential variables, such as slope, elevation, and the RUSLE equation parameters, have significantly contributed to enhancing the model's robustness by capturing the spatial dynamics influencing the studied phenomenon. The relative importance of these factors, as revealed in the previous analysis, has helped refine classification accuracy and minimize prediction errors.

Additionally, the tuning of key hyperparameters, including eta = 0.05, max_depth = 22, gamma = 0, subsample = 0.5, and colsample_bytree = 1, has ensured a well-balanced trade-off between bias and variance, reducing overfitting while maximizing model generalization. The optimized tree depth and adjusted data sampling have notably reinforced the model's ability to learn complex relationships without compromising prediction stability.

Finally, the shape of the ROC curve, characterized by a sharp rise toward the top-left corner, indicates that the model achieves high sensitivity with a low false positive rate. This result highlights the effectiveness of the adopted methodological choices, confirming that the XGBoost-based approach, combined with a rigorous variable selection and fine-tuned hyperparameter optimization, has led to a reliable and precise classification of the studied areas.
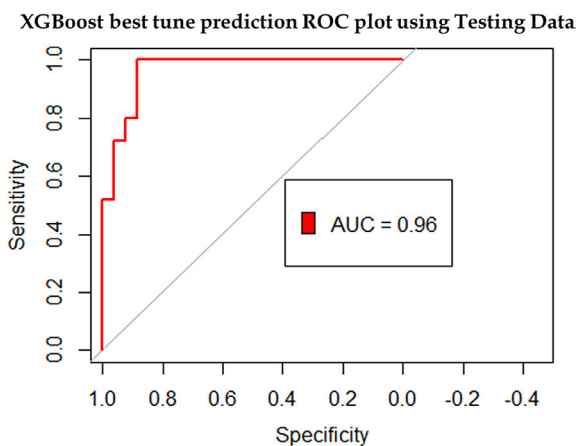
Sheet erosion susceptibility mapping

The sheet erosion susceptibility map, illustrated in Figure 10, presents the spatial distribution of erosion risk predicted using the optimized XGBoost model. The color gradient, ranging from black (low susceptibility) to yellow (high susceptibility), highlights the heterogeneity of erosion-prone areas within the study region. This mapping is primarily influenced by key environmental conditioning factors, particularly the parameters of the RUSLE equation, as well as topographic variables such as slope and elevation.

The results align with the variable importance analysis, which identified topographic factors as the dominant contributors to the
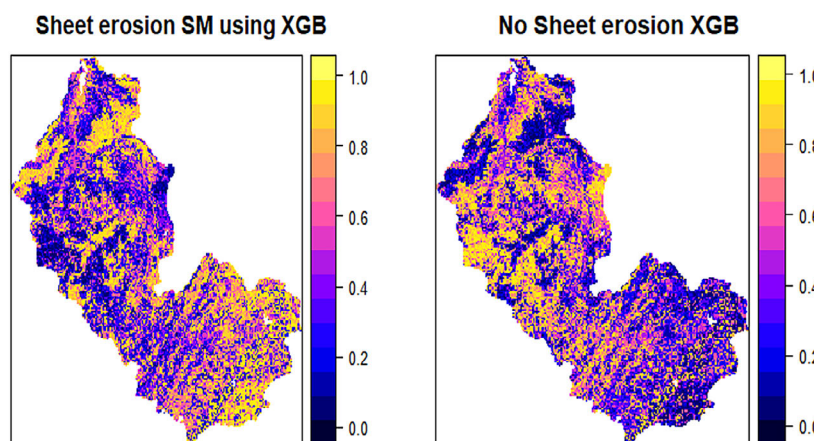

Figure 9. The ROC curve with AUC

Figure 10. Sheet erosion susceptibility map (XGBoost) for the Oued Beht watershed

erosion process. Specifically, high susceptibility zones are concentrated in areas with steep slopes and elevated terrains, where runoff intensity and soil instability are more pronounced. In contrast, low susceptibility areas correspond to flatter terrains, where erosion risk remains minimal.

The model's high predictive accuracy, reflected by a strong AUC ROC score, is attributed to the optimal tuning of hyperparameters, including those related to model learning, tree depth, regularization, and data sampling. This fine-tuning has significantly improved the model's generalization ability while mitigating overfitting, ensuring a robust and reliable spatial classification. These findings confirm that XGBoost, when combined with a rigorous selection of conditioning factors and a well-calibrated optimization process, serves as a powerful tool for mapping sheet erosion susceptibility. This approach provides valuable insights for environmental risk management and the development of effective soil conservation strategies.

The spatial distribution of sheet erosion, as illustrated by the PAP/CAR model and the susceptibility mapping using the XGBoost-based machine learning approach, reveals significant consistencies as well as notable differences. The PAP/CAR model classifies erosion forms based on observed geomorphological features, highlighting the dominance of sheet erosion (L1 and L2 classes) in the central and southeastern parts of the watershed. These areas correspond to moderate-to-steep slopes with heterogeneous lithology, particularly marl and clay formations, which are highly susceptible to surface runoff. The classification also identifies localized areas of more advanced erosion (L2D2) in the northern and northeastern regions, indicating zones where sheet erosion transitions into more severe linear erosion processes. However, this approach is largely based on expert-based classification and direct field observations, which may limit its capacity to capture fine-scale variations in erosion susceptibility.

In contrast, the XGBoost model generates a continuous susceptibility map based on machine learning predictions, providing a more detailed and probabilistic assessment of sheet erosion risk. The results indicate a strong agreement with the PAP/CAR model in terms of the general distribution of high-risk zones, particularly in the central and southeastern parts of the watershed. However, the machine learning model captures finer variations within these zones, highlighting micro-scale heterogeneity driven by slope gradient, land cover, and soil texture. The XGBoost model also extends high susceptibility predictions to additional areas in the northwest and near river networks, suggesting that these regions, though less highlighted in the PAP/CAR classification, could also be prone to sheet erosion under certain conditions.

Overall, while both approaches confirm the influence of topographic and lithological factors on erosion susceptibility, the machine learning model provides a more detailed spatial representation, benefiting from a data-driven approach that optimizes the weighting of different conditioning factors. The PAP/CAR model remains valuable for conceptualizing erosion processes but may require further refinement when applied to predictive mapping.

CONCLUSIONS

This study highlights the importance of integrating traditional erosion assessment methods with advanced machine learning models to enhance predictive accuracy. The comparative analysis of the PAP/CAR model and XGBoost underscores the strengths and limitations of each approach. While PAP/CAR effectively classifies erosion-prone zones based on geomorphological criteria, it may overestimate risk areas due to its reliance on expert-based classification. Conversely, the machine learning model refines spatial predictions by optimizing the weighting of key environmental factors, providing a more detailed and probabilistic erosion susceptibility map.

The results confirm that topographic factors, particularly slope and elevation, play a dominant role in erosion susceptibility, followed by soil properties and rainfall intensity. The high predictive performance of XGBoost, validated through cross-validation and ROC analysis, demonstrates its effectiveness in capturing complex spatial patterns of erosion risk. These findings support the integration of data-driven approaches in environmental risk assessment, offering valuable tools for decision-makers in soil conservation and watershed management.

REFERENCES

1. Achu, A. L., Jobin, T. (2023). Soil erosion and sediment yield modeling in a tropical mountain watershed of the southern Western Ghats, India using RUSLE and Geospatial tools. *Total Environment Research Themes* 8 (décembre):100072. https://doi.org/10.1016/j.totert.2023.100072

2. Ahmad, Mukhtar S., MonaLisa, Khan, S. (2023). Comparative analysis of analytical hierarchy process (AHP) and frequency ratio (FR) models for landslide susceptibility mapping in Reshun, NW Pakistan. *Kuwait Journal of Science* 50(3): 387–98. https://doi.org/10.1016/j.kjs.2023.01.004

3. Yacine, A.E, Oudija, F. Nassiri, L. Essahlaoui, A. (2019). Modélisation et cartographie des risques d'érosion hydrique du sol par l'application des SIG, télédétection et directives PAP/CAR. Cas du Bassin Versant de Beht, Maroc. *European Scientific Journal, ESJ* 15(12): 259–259. https://doi.org/10.19044/esj.2019.v15n12p259

4. Akalai, Noaman, Rachid Hlila, Mohamed El Imrani, et Chakib Darraz. (2014). Risk of water erosion in coastal watersheds North of Tetuan (Internel Rif, Northern Morocco): Evidences from GIS-Based *Spatial Approach.* 8(4).

5. Arnoldus, H. M. J. (1980). An approximation of the rainfall factor in the universal soil loss equation. *An Approximation of the Rainfall Factor in the Universal Soil Loss Equation.*, 127–32.

6. Ashiagbor, G., Forkuo, E. K., Laari, P., Aabeyir, R. (2013). Modeling soil erosion using rusle and GIS tools. *International Journal of Remote Sensing* 2(2319).

7. Ashiagbor, G., Forkuo, E. K., Laari, P., Aabeyir, R. (2012). Modeling soil erosion using RUSLE and GIS tools. *International Journal of Remote Sensing & Geoscience (IJRSG)* 2 (Juillet): 7–17.

8. Asmare, D., Hailemariam, T. (2021). Assessment of rock slope stability using slope stability probability classification system, around AlemKetema, North Shoa, Ethiopia. *Scientific African* 12 (Juillet):e00730. https://doi.org/10.1016/j.sciaf.2021.e00730

9. Basharat, M., Rohn, J., Baig, M. S., Khan, M. R. (2014). Spatial distribution analysis of mass movements triggered by the 2005 Kashmir earthquake in the Northeast Himalayas of Pakistan. *Geomorphology* 206 (février):203–14. https://doi.org/10.1016/j.geomorph.2013.09.025

10. Boissy, R., Ndiaye, M., Diatta, M., Mbaye, M. (2022). Utilisation d'un SIG pour l'évaluation et la cartographie des risques d'érosion hydrique par l'Equation Universelle des Pertes en sol Révisée (RUSLE) dans le Département de Saraya (Sénégal). *VertigO : la revue électronique en sciences de l'environnement* 22(2): 1–25. https://doi.org/10.4000/vertigo.38034

11. Boukrim, S., Lahrach, A., Midaoui, A., Benjelloun, F., Benabdelhadi, M., Lahrach, H., Chaouni, A. (2016). Cartographie De L' érosion qualitative des sols du bassin versant De L' Aoudour (Rif-Maroc). *European Scientific Journal* 12 (mai):1857–7881. https://doi.org/10.19044/esj.2016.v12n11p295

12. Bryan, R. B., Poesen, J. (1989). Laboratory experiments on the influence of slope length on runoff, percolation and rill development. *Earth Surface Processes and Landforms* 14(3): 211–31. https://doi.org/10.1002/esp.3290140304

13. Chalise, D., Kumar, L., Kristiansen, P. (2019). Soil Land Degradation by Soil Erosion in Nepal.

14. Dallahi, Y., El Aboudi, A., Sahel, Y., Aafi, A., El Mderssa, M., Malki, F. (2021). Evaluation de l'impact de la dynamique du couvert végétal sur l'érosion hydrique à l'aide de la méthode PAP/CAR et la télédétection spatiale dans le bassin versant de Kharouba (Plateau Central, Maroc). *Revue Marocaine des Sciences Agronomiques et Vétérinaires* 9(4): 562–66.

15. De Jong S. M. (1994). Applications of reflective remote sensing for land degradation studies in a Mediterranean environment. *GéoProdig, portail d'information géographique.*

16. Duchemin, M., Lachance, M., Lagacé, R., Majdoub, R. (2005). Variation spatiale et temporelle de l'érosion hydrique et du transport sédimentaire sur un petit bassin versant agricole. *Vecteur Environnement* 38:40–50.

17. Duiker, S. W, Flanagan, D. C., Lal, R. (2001). Erodibility and infiltration characteristics of five major soils of southwest Spain. *CATENA* 45 (2): 103–21. https://doi.org/10.1016/S0341-8162(01)00145-X

18. Efiong, J., Eni, D. I., Obiefuna, J. N., Etu, S. J. (2021). Geospatial modelling of landslide susceptibility in Cross River State of Nigeria. *Scientific African* 14 (novembre):e01032. https://doi.org/10.1016/j.sciaf.2021.e01032

19. El Amarty, F., Lahrach, A., Benaabidate, L., Chakir, A. (2024). Estimating soil erosion and sediment yield using geographic information system in the Central Pre-Rif (Northern Morocco) – The case of the Oued Leben watershed. *Ecological Engineering & Environmental Technology* 25 (8): 1–16. https://doi.org/10.12912/27197050/187977

20. EL Hadi, H. (2014). Evaluation et quantification de l'erosion et la sédimentation à partir des modèles RUSLE, MUSLE et déposition intégrés dans un SIG. Application au Sous-Bassin de l'Oued Sania (Bassin de Tahaddart, Rif nord occidental, Maroc) ». *European Journal of Scientific Research* 125 (octobre):57–178.

21. Elkadiri, R., Sultan, M., Youssef, A. M., Elbayoumi, T., Chase, R., Bulkhi, A. M., Al-Katheeri, M.M. (2014). A remote sensing-based approach for

debris-flow susceptibility assessment using artificial neural networks and logistic regression modeling. *IEEE Journal of Selected Topics in Applied Earth Observations and Remote Sensing* 7 (12): 4818–35. https://doi.org/10.1109/JSTARS.2014.2337273

22. Gebrehiwot, S. G., Bewket, W., Gärdenäs, A. I., Bishop, K. (2014). Forest cover change over four decades in the Blue Nile Basin, Ethiopia: Comparison of three watersheds. *Regional Environmental Change* 14 (1): 253–66. https://doi.org/10.1007/s10113-013-0483-x

23. HCEFLCD. (2014). Biodiversité et valeurs écologiques d'un tronçon de la basse vallée de l'Oued Beht situé entre les retenues de Barrages d'El Kansera et Ouljet Essoltane (Province de Khémisset - Maroc).

24. Hilmi, M., Mahamoud, A., El, M., Qninba, A. (2023). Biodiversity and ecological values of a part of the lower valley of Oued Beht located between the dams of El Kansera and Ouljet Essoltane (Province of Khemisset – Morocco) Biodiversité et valeurs écologiques d'un tronçon de la basse vallée de l'Oued Beht situé entre les retenues de Barrages d'El Kansera et Ouljet Essoltane (Province de Khémisset -Maroc). *Bulletin de l'Institut Scientifique*, mai, 7–17.

25. Iaaich, H., Moussadek, R., Baghdad, B., Mrabet, R., Douaik, A., Abdelkrim, D., Bouabdli A. (2016). Soil erodibility mapping using three approaches in the Tangiers province –Northern Morocco. *International Soil and Water Conservation Research* 4 (3): 159–67. https://doi.org/10.1016/j.iswcr.2016.07.001

26. Kusi, K. K., Khattabi, A., Mhammdi, N. (2023). Analyzing the impact of land use change on ecosystem service value in the main watersheds of Morocco. *Environment, Development and Sustainability* 25 (3): 2688–2715. https://doi.org/10.1007/s10668-022-02162-4

27. Lahlaoi, H., Rhinane, H., Hilali, A., Lahssini, S., Khalile, L. (2015). Potential erosion risk calculation using remote sensing and GIS in Oued El Maleh Watershed, Morocco. *Journal of Geographic Information System* 7 (2): 128–39. https://doi.org/10.4236/jgis.2015.72012

28. Lakhili, F., Benabdelhadi, M., Chaouni, A., Bouderka, N., Lahrach, A. (2017). Cartographie de l'érosion qualitative des sols du bassin versant de Beht (Maroc). *American Journal of Innovative Research and Applied Sciences* 4 (5): 174–85.

29. Maidment DR. 1993. Handbook of Hydrology.

30. Mesrar, H., Sadiki, A., Navas, A., Faleh, A., Quijano, L., Chaaouan, J. (2015). Modélisation de l'érosion Hydrique et Des Facteurs Causaux, Cas de Oued Sahla, Rif Central, Maroc. *Zeitschrift Für Geomorphologie* 59 (4): 495.

31. Mohajane, M., Costache, R., Karimi, F., Pham, Q. B., Essahlaoui, A., Nguyen, H., Laneve, G., Oudija, F. (2021). Application of remote sensing and machine learning algorithms for forest fire mapping in a Mediterranean area. *Ecological Indicators* 129 (octobre):107869. https://doi.org/10.1016/j.ecolind.2021.107869

32. Ousmana, H., El Hmaidi, A., Essahlaoui, A., Bekri, H., Ouali, E. A. (2017). Modélisation et cartographie du risque de l'érosion hydrique par l'application des SIG et des directives PAP/CAR. Cas du bassin versant de l'Oued Zgane (Moyen Atlas tabulaire, Maroc). *Bulletin de l'Institut Scientifique, Rabat, Section Sciences de la Terre* 39:103–19.

33. Ozer, B. C., Mutlu, B., Nefeslioglu, H. A., Sezer, E. A., Rouai, M., Dekayir, A., Gokceoglu, C. (2020). On the use of hierarchical fuzzy inference systems (HFIS) in expert-based landslide susceptibility mapping: The central part of the Rif Mountains (Morocco). *Bulletin of Engineering Geology and the Environment* 79 (1): 551–68. https://doi.org/10.1007/s10064-019-01548-5

34. Pelletier, J. D. (2012). A spatially distributed model for the long-term suspended sediment discharge and delivery ratio of Drainage Basins. *Journal of Geophysical Research: Earth Surface* 117 (F2): 2011JF002129. https://doi.org/10.1029/2011JF002129

35. Renard, K. G., Foster, G. R., Weesies, G. A., Porter, J. P. (1991). RUSLE: Revised Universal Soil Loss Equation. *Journal of Soil and Water Conservation* 46 (1): 30–33.

36. Sadiki, A., Mesrar, H., Faleh, A., Chaaouan, A. (2012). Modelisation et cartographie des risques de l'erosion hydrique: cas du bassin versant de l'Oued Larbaa, Maroc. *Papeles de Geografía.*

37. Tabyaoui, M, Tahiri, H., Hadi, E., Hammichi, E., Achab, F., Tahiri, M., Hassan, T., et al. (2016). Modelling soil erosion and sedimentation in the Oued Haricha Sub-Basin (Tahaddart Watershed, Western Rif, Morocco): Risk Assessment. *Journal of Geoscience and Environment Protection* 4 (février):107–19. https://doi.org/10.4236/gep.2016.41013

38. Tahouri, H., Sadiki, A., Karrat, L., Johnson, V. C., Ngai, W. C. (2022). Using a modified PAP/RAC model and GIS-for mapping water erosion and causal risk factors: Case study of the Asfalou Watershed, Morocco. *International Soil and Water Conservation Research* 10 (2): 254–72. https://doi.org/10.1016/j.iswcr.2021.07.003

39. Tahouri, J., Sadiki, A., Karrat, L., Mesrar, H., Johnson, V. C. (2019). Tahouri: Using PAP/RAC model and GIS tools for mapping and study of water erosion processes in the Mediterranean environment: Case of the Asfalou watershed.

40. Toy, T. J., Foster, G. R., Renard, K. G. (1999). RUSLE for Mining, Construction and Reclamation Lands. *Journal of Soil and Water Conservation* 54 (2): 462–67.